Abnormal Microenvironment Responsive MRI Nanoprobe

Magnetic resonance imaging (MRI) is often used to diagnose diseases due to its high spatial, temporal and soft tissue resolution. Environment-responsive or smart MRI nanoprobes can specifically target cells based on differences in the cellular environment and improve the contrast between diseased tissues and normal tissues.

Keywords: MRI nanoprobe ; environment responsive ; design ; application

1. Introduction

Molecular imaging uses molecular probes for specific biological targets in the tumor microenvironment to obtain better 3D images regarding the anatomical structure, physiology, pathology, etc., which can provide an important reference basis for early and accurate tumor diagnosis and treatment. In the tumor microenvironment, metabolic, immune and endocrine changes affect the occurrence and development of tumors. Researchers have synthesized targeted molecular probes for specific and highly expressed receptors on neovascular endothelial cells and tumor cells to investigate the occurrence and development of tumors and their structural characteristics at the microscopic level [1]. This targeting molecular probe contains three parts: targeting ligand, transporter, and contrast agent, and it should have an amplifying effect, strong penetrating ability, long half-life, and rapid elimination from the body [2].

Nanoparticles (NPs) play an important role in the medical field by virtue of their unique nanoscale characteristics and their core or surface-modified functional groups. By introducing multiple modes into NPs, they can effectively act as imaging contrast agents and can provide complementary information for accurate cancer diagnosis. Most traditional anti-cancer drugs cannot distinguish between normal cells and cancer cells; however, NPs can preferentially accumulate in the tumor area via the enhanced penetration and retention effects (EPR), and can effectively carry and transport imaging probes, therapeutic agents, or biological materials to specific locations, such as specific organs, tissues, and even cells [3]. The composition of the tumor microenvironment is quite different from that of normal tissues. Efficient and selective nanoprobes can help in realizing real-time in situ cell imaging and enable non-invasive cancer treatment in response to tumor microenvironment (hypoxia, slightly acidic, redox, enzyme) or external field stimulation response (light, heat, and magnetism). In recent years, there has been a rapid development of environment-responsive MRI probes. They have stimulus response capabilities and can specifically target cells based on the different characteristics of the cell environment. This significantly increases the cumulative release rate of nanomolecular imaging probes, improves the in vivo imaging efficiency and drug availability, and improves the tracer SNR between the diseased sites and normal tissues [4].

2. The Design of the MRI Nanoprobe

2.1. pH-Responsive MRI Nanoprobes

Tumor tissues grow and metabolize rapidly by consuming large amounts of glucose and oxygen, resulting in the accumulation of excessive lactic acid and hydrogen ions in the extracellular fluid. This makes the tumor microenvironment to be weakly acidic (pH 5.5 to 6.8) [5][6]. Thus, the pH-responsive MRI probes can be designed in the following two ways: (1) the probe cleaves and releases ions automatically in response to changes in the environmental pH; (2) the probe changes its shape in response to changes in the environmental pH changes, such as becoming smaller, bigger, or "disintegrate" [7].

Yua et al. designed two pH-sensitive MRI/FI bimodal agents based on AuNPs (Figure 1). The first (Au@Gd and Au@Gd&RGD) contained rhodamine derivatives that were sensitive to acidic conditions, which facilitated the monitoring of the impact of pH changes of lysosomes in living cells. The second (D-Au@Gd and D-Au@Gd&RGD) included two pH-

responsive fluorophores, rhodamine and fluorescein derivatives, which could provide a very accurate intracellular pH map and could also be used to calculate the pH of living cells.
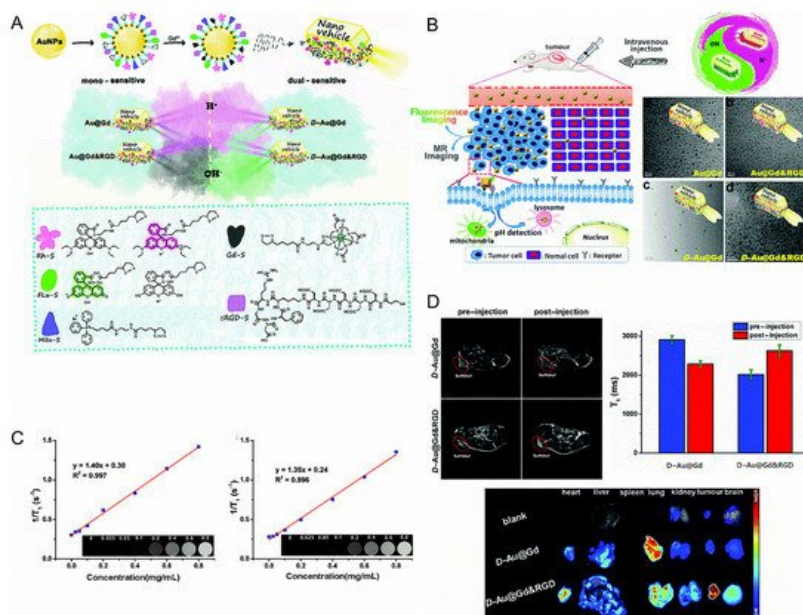

Figure 1. (**A**): Schematic diagram of the nanovehicles. (**B**): Schematic diagram of the nanovehicles and TEM images. (**C**): (Left) in vitro T_1-weighted MR imaging of D-Au@Gd in PBS, (Right) in vitro T_1-weighted MR imaging of D-Au@Gd&RGD in PBS. (**D**): (Upper left) the MRI of D-Au@Gd and D-Au@Gd&RGD in U87 tumor-bearing nude mice, (Upper right) the fluorescence imaging, (Lower) the semi-quantitative MRI signal intensity in solid tumors [8]. Reproduced with permission from Royal Society of Chemistry 2020.

2.2. Enzyme-Responsive MRI Nanoprobes

Some of the enzymes, such as matrix metalloproteinase, esterase, amylase and cathepsin B, are overexpressed both outside and inside the tumor cells. Caspase-3/7 is a marker of apoptosis. Rao et al. formed Gd NPs that exhibited an r_1 increasing effect after interaction with caspase-3/7 by regulating self-assembly and macrocyclization. The nanoprobe they synthesized called C-SNAM is composed of a Gd-DOTA complex that is connected to the DEVD peptide, the disulfide bond sensitive to GSH, and the self-assembly of 2-cyano-6-hydroxyquinoline and D-cysteine residues. In the GSH-induced reducing environment inside the cell, cyclization is caused by the degradation of DEVD peptide in the presence of caspase-3/7. The amplification of r_1 in Gd NPs and the tissue retention due to the increase in size enhances the T_1 contrast in MRI. They used this nanoprobe to detect caspase-3/7 activity in a chemically sensitive tumor model and successfully completed in vitro and in vivo imaging. Next, they compared it with a nanoprobe that could not be circularized [9]. Coincidentally, after intra-articular injection of matrix-related stem cells, a similar method was used to detect stem cell apoptosis, which could treat cartilage defects [10].

2.3. Redox-Responsive MRI Nanoprobes

Fu et al. reported a new ^{19}F-MRI contrast agent, a branched-chain fluorinated glycoprotein, which could target cancer imaging in response to a reducing environment (Figure 2). In the presence of disulfide-containing crosslinking monomers, one-pot RAFT polymerization of glucose and fluoro-monomers could easily prepare fluoro-glycoproteins. Since fluorinated sugar polymers interacted with sugar transporters overexpressed on the cell surface, the binding of glucose units along the polymer chain allowed them to effectively target cancer cells. Additionally, the polymer exhibited enhanced ^{19}F-MRI signal under reduced conditions [11].
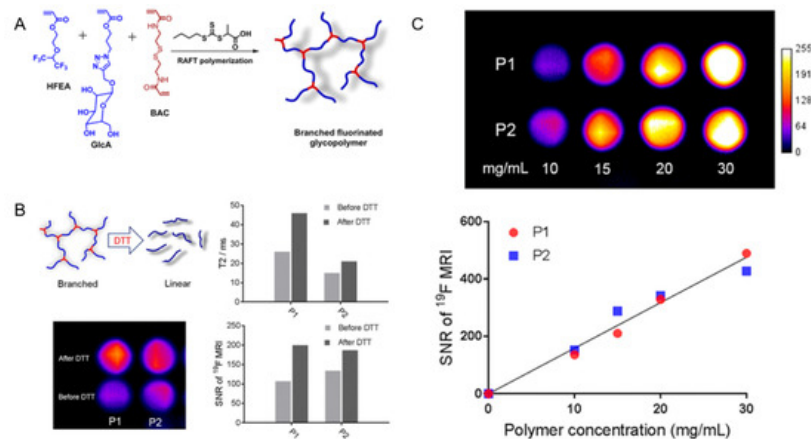
Figure 2. (**A**): Synthesis of branched fluorinated glycopolymers by a one-pot RAFT Polymerization. (**B**): (Upper left) the transformation of a branched structure to a linear structure when the polymer is exposed to high levels of DTT; (Upper right) a comparison of the T_2 relaxation time of P1 and P2 before and after treatment with 10 mM DTT; (Lower left) a comparison of ^{19}F-MRI images of P1 and P2 solutions before and after 10 mM DTT treatment; (Lower right) the signal-to-noise ratio of ^{19}F-MRI of P1 and P2 solutions before and after 10 mM DTT treatment. (**C**): (Upper) the ^{19}F-MRI of P1 and P2 solutions; (Lower) the ^{19}F-MRI signal-to-noise ratio of P1 and P2 solutions within a certain concentration range [11]. Reproduced with permission from American Chemical Society 2019.

2.4. Other Examples of MRI Nanoprobes

Table 1 summarizes the design of the environment-responsive MRI nanoprobes mentioned in the review, including the name of the probes and the resulting effect.

Table 1. Summary of the design of environment-responsive MRI nanoprobes.

	Probe	Consequence and Effect	Ref.
pH-responsive MRI nanoprobes	PEGMnCaP	It dissolved at an acidic pH, and the released Mn^{2+} could combine with the proteins, increasing the T_1 contrast.	[12]
	ATO@SiO$_2$ NPs	The acidic medium triggered the simultaneous release of the clinical anticancer drug ATO and Mn^{2+}, enhancing the contrast of T_1.	[13]
	MnO NPs @SiO$_2$	In an acidic environment, Mn^{2+} was released, enhancing T_1 contrast.	[14]
	MnOx-HMCNs	A mildly acidic solution could increase its T_1 relaxation value by 52.5 times. It showed an anti-metastatic effect and high performance in reversing cancer cell multi-drug resistance.	[15]
	Fe$_3$O$_4$ NPs @Micelles	At pH < 6.8, the micelle ruptured, releasing the iron oxide NPs and enhancing the T_2 contrast.	[16]
	^{19}F-Peptide nanostructures	In an acidic environment, due to the increased mobility of fluorine probes in cylindrical nanostructures, their arrangement was cylindrical, turning the ^{19}F-MRI signal "on".	[17]
	Au NPs @mesoporous SiO$_2$ NPs	At pH < 6, the hydrazine bond was hydrolyzed and the fluorine nanoprobe was released, consequently activating the ^{19}F-MRI signal.	[18]
	^{19}F-Micelles	By decomposing the micelles, it could achieve pH-based environmental response and qualitative measurement of the environmental pH values by responding to ^{19}F-MRI.	[19]
	GdNP-DO3A	The nitrophenol group was protonated at low pH, allowing water to approach Gd. An increase in pH caused an increase in the relaxation performance.	[20]
	Au@Gd&RGD	It could be used to monitor pH changes of lysosomes in living cells due to its sensitivity to acidic conditions.	[8]
	D-Au@Gd&RGD	It could obtain a precise intracellular pH map and quantitatively calculate the pH values of living cells.	[8]
	GMF&drug molecules @NPs	Under acidic conditions, the hydrophobic-hydrophilic transition of the pH-responsive polymer caused the amplification of the MRI signal, resulting in the rapid release of the drug.	[21]

Probe	Consequence and Effect	Ref.
Enzyme-responsive MRI nanoprobes		
C-SNAM	In the reducing environment of GSH in the cell, cyclization was triggered by the degradation of DEVD peptide in the presence of caspase 3/7. The amplification of r_1 in Gd NPs and the tissue retention due to the increase in size caused T_1 contrast enhancement in MRI.	[9]
Gd chelate-^{19}F	When the peptide was cleaved by caspase 3/7, the Gd chelate was separated from fluorine, and the ^{19}F-MRI signal was turned on.	[22] [23]
fluorinated hydrogel precursor	Tyrosine kinase controlled the decomposition of the hydrogel and subsequent turning-on of the ^{19}F-MRI signal.	[24]
Gd-peptide	When the nanoprobe interacted with PDI, the nanoprobe bound to fibrin, increasing r_1 by 70%.	[25]
Gadoteridol@liposomes	In the presence of PLA_2, liposomes were degraded and Gd probes were released, leading to a significant reduction in T_1 relaxation time.	[26]
IO NPs (MMP-9)	After MMP-9 sheared the IO, it released the PEG molecule, enhancing the T_2 relaxation effect.	[27]
IO NPs (MMP-14)	At the tumor site, MMP-14 cleavage of the peptide, resulting in the accumulation of nanoprobes in the tumor and enhancing the T_2 contrast.	[28]
Salicylic acid derivative	Sulfatase and esterase cleaved the probe, turning the CEST signal "on"	[29]
Redox-responsive MRI nanoprobes		
$Fe_3O_4@Mn_3O_4$	In the presence of GSH, the shell decomposed into Mn^{2+} exposing iron oxide NPs and increasing r_1 and r_2.	[30]
^{19}F-Fe^{3+} chelate	When APS oxidized Fe^{2+} to Fe^{3+}, the signal was turned "off". A mild reducing agent could reduce the system to Fe^{2+} turning the signal "on" again.	[31]
Gd chelate–SiO_2 NPs	The presence of GSH could separate Gd chelate from SiO_2, significantly increasing r1.	[32]
^{19}F@SiO_2-Gd-chelate	The reducing environment could not only break the disulfide bond but also separate the Gd chelate from the fluorine probe, thereby turning the ^{19}F-MRI signal "on".	[33]
CuL_1 and CuL_2	They retained their initial quenched ^{19}F-MRI signal. When the complex was reduced, the signal increased.	[34]
Cu^{2+} ATSM derivatives	Adjusting the distance between Cu^{2+} and F atoms could enhance ^{19}F-MRI relaxation.	[35]
Branched fluorinated glycoprotein	In a reducing environment, the polymer exhibited an enhanced ^{19}F-MRI signal.	[11]
Other examples of MRI nanoprobes		
Ce6/Fe_3O_4-M	The elemental oxygen generated by light irradiation triggered the cleavage of TK, obtaining a negatively enhanced T_2-weighted MRI signal.	[36]
Apt-TDNs-GdHAp	TDNs enhanced the monodispersity of the nanoprobe and improved the stability and accessibility of targeted tumors.	[37]
CCRM	1,8 and 1,4-isomers had paramagnetically shifted amide protons, which acted as excellent pH probe.	[38]
GD-CHyD	The increased reactivity and affinity of Gd-CHyD could improve the contrast between the lung and the liver.	[39]
Tm-PFZ-1	Tm^{3+} could eliminate the ^{19}F-MRI signal; chelation of Zn^{2+} could provide ^{19}F-MRI signal.	[40]
inorganic probe-Ni^{2+}	It increased the ^{19}F-MRI relaxation rate. This nanoprobe could detect light or enzyme expression in living cells.	[41]

3. The Application of the MRI Nanoprobe

Molecular nanoprobes have good targeting ability, high SNR, and deep tissue in situ imaging. They are important tools for tumor diagnosis and treatment. Since MRI technology has strong penetrating power and high spatial resolution, it is often used to monitor the drug transport process in organisms, combining MRI and molecular nanoprobes to design an

environment-responsive nanoprobe that could remove background interference when imaging deep tissues in tumor detection and imaging.

Gao et al. modified Fe_3O_4 NPs using in situ cross-linking reactive peptide sequences to achieve enhanced tumor imaging (Figure 3). The tumor-specific Arg-Gly-Asp peptide and the self-peptide were connected by disulfide bonds. In the tumor environment, peptides were cleaved using glutathione, facilitating the reaction between the exposed thiol groups and the maleimide groups located in adjacent particles. The labeling responsive particle nanoprobes with ^{99m}TC, combined with the aggregation of Fe_3O_4 NPs triggered by the tumor microenvironment resulted in the enhancement of the T_2 effect, it had anti-phagocytic surface coating, active targeting ability, and dual-mode imaging [42].
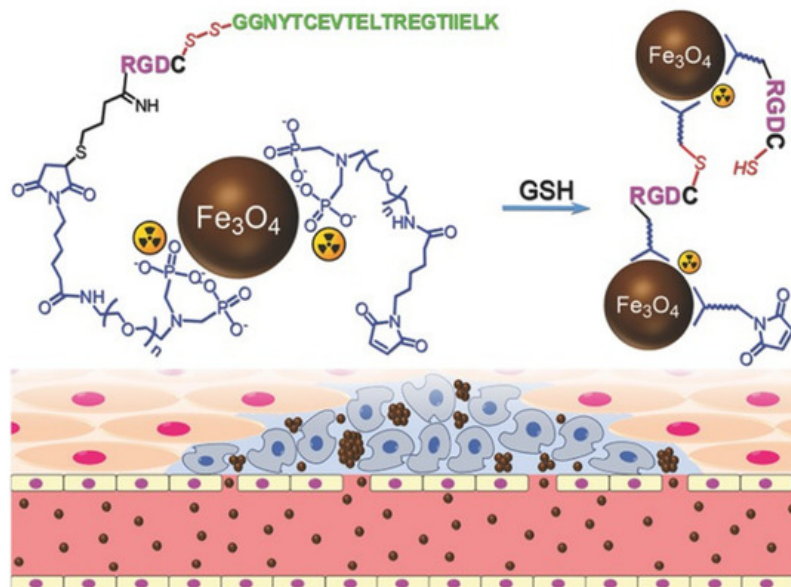

Figure 3. The design of ^{99m}Tc-labeled anti-phagocytosis Fe_3O_4 nanoparticles and the cross-linking reaction between the particles to trigger the formation of particle aggregation in the tumor microenvironment by GSH [42]. Reproduced with permission from Wiley-VCH GmbH, Weinheim 2017.

Peng et al. used a phospholipid monolayer to coat molecules containing 27 fluorine atoms, fluorine-containing chelating agents and BODIPY fluorescent dyes, obtaining a highly stable and highly biocompatible bimodal nanoprobe for cell labeling [43] (Figure 4).
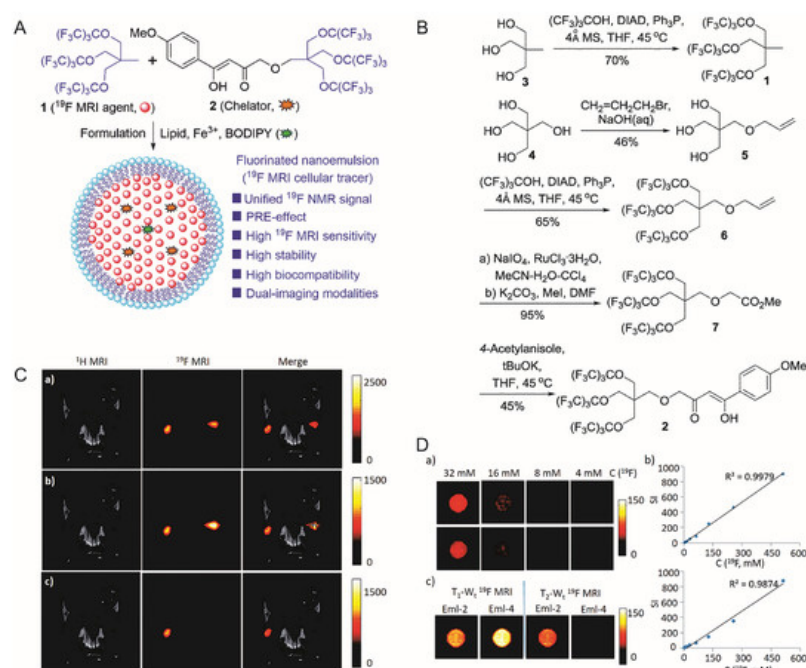

Figure 4. (**A**): Design of the nanoemulsion as ^{19}F-MRI cellular tracer. (**B**): Synthesis of ^{19}F-MRI agent 1 and chelator 2. (**C**): In vivo, ^{19}F-MRI tracking of Eml-2- and Eml-4-labeled RAW264.7 cells in mice. (Upper) ^{19}F density MRI; (Middle) T_1-weighted ^{19}F-MRI; (Lower) T_2-weighted ^{19}F-MRI; (Left) Eml-2-labeled cells were injected; (Right) Eml-4 labeled cells were injected for comparison. (**D**): (Upper left, middle left) ^{19}F density MRI of Eml-2 and Eml-4, respectively; (Right) is SI versus $C(^{19}F)$ of Eml-2 and Eml-4, respectively; (Lower left) ^{19}F T_1/T_2-W_t MRI of Eml-2 and Eml-4 at 9.4T. [43]. Reproduced with permission from Royal Society of Chemistry 2018.

Table 2 summarizes the application of the environment-responsive MRI nanoprobes mentioned in the review.

Table 2. Summary of the application of environment responsive MRI nanoprobes.

Probe	Application	Ref.
adriamycin@vesicles	They can be used to trace liposome drug delivery systems and ensure the mobility of fluorine containing fragments and provide better ^{19}F-MRI signals.	[44]
Fe$_3$O$_4$@Au-DOX-mPEG/PEG-FANPs	They can realize the dual role of tumor imaging and treatment.	[45]
HB-pGAEMA-RGD-GD	The nanoprobe has been shown to significantly enhance the MRI signal intensity at the tumor site in vivo.	[46]
Arg-Gly-Asp Fe$_3$O$_4$ NPs	They can enhance the T$_2$ effect and possess anti-phagocytic surface coating, active targeting ability, and dual-mode imaging.	[42]
TFPDA	They have higher imaging sensitivity and specificity, and provide strong support for the early diagnosis of AD.	[47] [48]
phospholipid coat molecules	They can prepare highly stable and highly biocompatible bimodal nanoprobes for cell labeling.	[43]
5-fluorouracil &Au NPs	In the presence of target DNA in the system, the fluorine-containing base DNA is released, restoring the signal.	[49]
^{19}F-DNA polymer	They serve as an anchor point to graft partially complementary fluorine-labeled DNA.	[50]
ER molecules probes	They have a targeted imaging effect in the lesions with ER-positive expression.	[51]

4. Summary

MRI is undergoing a fast transformation from traditional non-specific physical imaging to specific molecular and gene-level imaging. Disease evaluation indicators are also changing from traditional morphological changes and anatomical positioning to changes in enzyme function, receptor levels, and gene expression. MR molecular imaging is known to provide a more comprehensive, 3D, specific imaging and biological data for diseases, and shows broad application prospects in life sciences, basic medicine, and clinical research. The diseased tissue microenvironment is significantly different from normal tissues. Thus, using the physical and chemical properties of the diseased tissues to develop environment-responsive MRI nanoprobes can not only improve the imaging effect of the tumors, but also assist in disease treatment. From an imaging point of view, achieving the clinical transformation of environment-responsive nanoprobes requires improving the sensitivity of MRI. Thus, the current strategy aims to obtain a good signal-to-noise ratio with a longer scan time. Future studies might focus on improving material design to improve sensitivity. MR molecular imaging would further facilitate the diagnosis and treatment of diseases; however, we should also strive to improve the deficiencies that still exist in MR molecular imaging, such as nanoprobe safety, imaging sensitivity, etc.

References

1. Jun, H.Y.; Yin, H.H.; Kim, S.H.; Park, S.H.; Kim, H.S.; Yoon, K.H. Visualization of tumor angiogenesis using MR imaging contrast agent Gd-DTPA-anti-VEGF receptor 2 antibody conjugate in a mouse tumor model. Korean J. Radiol. 2010, 11, 449–456.

2. Tan, M.; Burden-Gulley, S.M.; Li, W.; Wu, X.; Lindner, D.; Brady-Kalnay, S.M.; Gulani, V.; Lu, Z.R. MR molecular imaging of prostate cancer with a peptide-targeted contrast agent in a mouse orthotopic prostate cancer model. Pharm. Res. 2012, 29, 953–960.

3. Torchilin, V. Tumor delivery of macromolecular drugs based on the EPR effect. Adv. Drug Deliv. Rev. 2011, 63, 131–135.

4. Zhu, J.; He, K.; Dai, Z.; Gong, L.; Zhou, T.; Liang, H.; Liu, J. Self-Assembly of Luminescent Gold Nanoparticles with Sensitive pH-Stimulated Structure Transformation and Emission Response toward Lysosome Escape and Intracellular Imaging. Anal. Chem. 2019, 91, 8237–8243.

5. Webb, B.A.; Chimenti, M.; Jacobson, M.P.; Barber, D.L. Dysregulated pH: A perfect storm for cancer progression. Nat. Rev. Cancer 2011, 11, 671–677.

6. Zhang, X.; Lin, Y.; Gillies, R.J. Tumor pH and its measurement. J. Nucl. Med. 2010, 51, 1167–1170.

7. Monica, C. Activatable probes for diagnosis and biomarker detection by MRI. J. Mater. Chem. B 2017, 5, 4332–4347.

8. Kang-Kang, Y.; Kun, L.; Chun-Yan, L.; Yong-Mei, X.; Yan-Hong, L.; Qian, Z.; Jin-Ku, B.; Xiao-Qi, Y. Multifunctional gold nanoparticles as smart nanovehicles with enhanced tumour-targeting abilities for intracellular pH mapping and in vivo MR/fluorescence imaging. Nanoscale 2020, 12, 2002–2010.

9. Ye, D.; Shuhendler, A.J.; Pandit, P.; Brewer, K.D.; Tee, S.S.; Cui, L.; Tikhomirov, G.; Rutt, B.; Rao, J. Caspase-responsive smart gadolinium-based contrast agent for magnetic resonance imaging of drug-induced apoptosis. Chem. Sci. 2014, 4, 3845–3852.

10. Nejadnik, H.; Ye, D.; Lenkov, O.D.; Donig, J.S.; Martin, J.E.; Castillo, R.; Derugin, N.; Sennino, B.; Rao, J.; Daldrup-Link, H. Magnetic resonance imaging of stem cell apoptosis in arthritic joints with a caspase activatable contrast agent. ACS Nano 2015, 9, 1150–1160.

11. Changkui, F.; Joyce, T.; Aidan, P.; Tianqing, L.; Cheng, Z.; Xiao, T.; Felicity, H.; Hui, P.; Whittaker, A.K. Fluorinated Glycopolymers as Reduction-responsive 19F MRI Agents for Targeted Imaging of Cancer. Biomacromolecules 2019, 20, 2043–2050.

12. Mi, P.; Kokuryo, D.; Cabral, H.; Wu, H.; Terada, Y.; Saga, T.; Aoki, I.; Nishiyama, N.; Kataoka, K. A pH-activatable nanoparticle with signal-amplification capabilities for non-invasive imaging of tumour malignancy. Nat. Nanotechnol. 2016, 11, 724–730.

13. Zhao, Z.; Wang, X.; Zhang, Z.; Zhang, H.; Liu, H.; Zhu, X.; Li, H.; Chi, X.; Yin, Z.; Gao, J. Real-time monitoring of arsenic trioxide release and delivery by activatable T(1) imaging. ACS Nano 2015, 9, 2749–2759.

14. Hsu, B.Y.; Ng, M.; Tan, A.; Connell, J.; Roberts, T.; Lythgoe, M.; Zhang, Y.; Wong, S.Y.; Bhakoo, K.; Seifalian, A.M.; et al. pH-Activatable MnO-Based Fluorescence and Magnetic Resonance Bimodal Nanoprobe for Cancer Imaging. Adv. Healthc. Mater. 2016, 5, 721–729.

15. Kim, H.J.; Matsuda, H.; Zhou, H.; Honma, I. Ultrasound-Triggered Smart Drug Release from a Poly(dimethylsiloxane)–Mesoporous Silica Composite. Adv. Mater. 2006, 18, 3083–3088.

16. Yang, H.Y.; Jang, M.S.; Gao, G.H.; Lee, J.H.; Lee, D.S. pH-Responsive biodegradable polymeric micelles with anchors to interface magnetic nanoparticles for MR imaging in detection of cerebral ischemic area. Nanoscale 2016, 8, 12588–12598.

17. Preslar, A.T.; Tantakitti, F.; Park, K.; Zhang, S.; Stupp, S.I.; Meade, T.J. (19)F Magnetic Resonance Imaging Signals from Peptide Amphiphile Nanostructures Are Strongly Affected by Their Shape. ACS Nano 2016, 10, 7376–7384.

18. Chen, S.; Yang, Y.; Li, H.; Zhou, X.; Liu, M. pH-Triggered Au-fluorescent mesoporous silica nanoparticles for 19F MR/fluorescent multimodal cancer cellular imaging. Chem. Commun. (Camb) 2014, 50, 283–285.

19. Huang, X.; Huang, G.; Zhang, S.; Sagiyama, K.; Togao, O.; Ma, X.; Wang, Y.; Li, Y.; Soesbe, T.C.; Sumer, B.D.; et al. Multi-chromatic pH-activatable 19F-MRI nanoprobes with binary ON/OFF pH transitions and chemical-shift barcodes. Angew. Chem. Int. Ed. Engl. 2013, 52, 8074–8078.

20. Mac Manus, M.P.; Hicks, R.J. The role of positron emission tomography/computed tomography in radiation therapy planning for patients with lung cancer. Semin Nucl. Med. 2012, 42, 308–319.

21. Wang, S.; Zhou, Z.; Wang, Z.; Liu, Y.; Jacobson, O.; Shen, Z.; Fu, X.; Chen, Z.Y.; Chen, X. Gadolinium Metallofullerene-Based Activatable Contrast Agent for Tumor Signal Amplification and Monitoring of Drug Release. Small 2019, 15, 1900691.

22. Mizukami, S.; Takikawa, R.; Sugihara, F.; Hori, Y.; Tochio, H.; Walchli, M.; Shirakawa, M.; Kikuchi, K. Paramagnetic relaxation-based 19f MRI probe to detect protease activity. J. Am. Chem. Soc. 2008, 130, 794–795.

23. Yue, X.; Wang, Z.; Zhu, L.; Wang, Y.; Qian, C.; Ma, Y.; Kiesewetter, D.O.; Niu, G.; Chen, X. Correction to "Novel (19)F Activatable Probe for the Detection of Matrix Metalloprotease-2 Activity by MRI/MRS". Mol. Pharm. 2017, 14, 1317–1318.

24. Zheng, Z.; Sun, H.; Hu, C.; Li, G.; Liu, X.; Chen, P.; Cui, Y.; Liu, J.; Wang, J.; Liang, G. Using "On/Off" (19)F NMR/Magnetic Resonance Imaging Signals to Sense Tyrosine Kinase/Phosphatase Activity in Vitro and in Cell Lysates. Anal. Chem. 2016, 88, 3363–3368.

25. Loving, G.S.; Caravan, P. Activation and retention: A magnetic resonance probe for the detection of acute thrombosis. Angew. Chem. Int. Ed. Engl. 2014, 53, 1140–1143.

26. Cheng, Z.; Tsourkas, A. Monitoring phospholipase A(2) activity with Gd-encapsulated phospholipid liposomes. Sci. Rep. 2014, 4, 6958.

27. Eyk, S.; Franziska, R.; Carsten, W.; Matthias, T.; Bernd, H.; Jörg, S. Protease-specific nanosensors for magnetic resonance imaging. Bioconjugate Chem. 2008, 19, 2440–2445.

28. Ansari, C.; Tikhomirov, G.A.; Hong, S.H.; Falconer, R.A.; Loadman, P.M.; Gill, J.H.; Castaneda, R.; Hazard, F.K.; Tong, L.; Lenkov, O.D.; et al. Development of novel tumor-targeted theranostic nanoparticles activated by membrane-type matrix metalloproteinases for combined cancer magnetic resonance imaging and therapy. Small 2014, 10, 566–575.

29. Daryaei, I.; Ghaffari, M.M.; Jones, K.M.; Pagel, M.D. Detection of Alkaline Phosphatase Enzyme Activity with a CatalyCEST MRI Biosensor. ACS Sens. 2016, 1, 857–861.

30. Kim, M.H.; Son, H.Y.; Kim, G.Y.; Park, K.; Huh, Y.M.; Haam, S. Redoxable heteronanocrystals functioning magnetic relaxation switch for activatable T1 and T2 dual-mode magnetic resonance imaging. Biomaterials 2016, 101, 121–130.

31. Tanaka, K.; Kitamura, N.; Takahashi, Y.; Chujo, Y. Reversible signal regulation system of 19F NMR by redox reactions using a metal complex as a switching module. Bioorg. Med. Chem. 2009, 17, 3818–3823.

32. Munoz Ubeda, M.; Carniato, F.; Catanzaro, V.; Padovan, S.; Grange, C.; Porta, S.; Carrera, C.; Tei, L.; Digilio, G. Gadolinium-Decorated Silica Microspheres as Redox-Responsive MRI Probes for Applications in Cell Therapy Follow-Up. Chemistry (Weinheim an der Bergstrasse, Germany) 2016, 22, 7716–7720.

33. Nakamura, T.; Matsushita, H.; Sugihara, F.; Yoshioka, Y.; Mizukami, S.; Kikuchi, K. Activatable 19F MRI nanoparticle probes for the detection of reducing environments. Angew. Chem. Int. Ed. Engl. 2015, 54, 1007–1010.

34. Kadakia, R.T.; Da, X.; Hongyu, G.; Bailey, B.; Meng, Y.; Que, E.L. Responsive fluorinated nanoemulsions for 19F magnetic resonance detection of cellular hypoxia. Dalton Trans. 2020, 49, 16419–16424.

35. Xie, D.; Kim, S.; Kohli, V.; Banerjee, A.; Yu, M.; Enriquez, J.S.; Luci, J.J.; Que, E.L. Hypoxia-Responsive (19)F MRI Probes with Improved Redox Properties and Biocompatibility. Inorg. Chem. 2017, 56, 6429–6437.

36. Deng, K.; Wu, B.; Wang, C.X.; Wang, Q.; Yu, H.; Li, J.M.; Li, K.H.; Zhao, H.Y.; Huang, S.W. An Oxidation-Enhanced Magnetic Resonance Imaging Probe for Visual and Specific Detection of Singlet Oxygen Generated in Photodynamic Cancer Therapy In Vivo. Adv. Healthc. Mater. 2020, 9, e2000533.

37. Yaqin, H.; Caizhi, L.; Xiandeng, H.; Lan, W. Mono-dispersed nano-hydroxyapatite based MRI probe with tetrahedral DNA nanostructures modification for in vitro tumor cell imaging. Anal. Chim. Acta 2020, 1138, 141–149.

38. Bond, C.J.; Cineus, R.; Nazarenko, A.Y.; Spernyak, J.A.; Morrow, J.R. Isomeric Co(ii) paraCEST agents as pH responsive MRI probes. Dalton Trans. 2020, 49, 279–284.

39. Akam, E.A.; Eric, A.; Rotile, N.J.; Slattery, H.R.; Zhou, I.Y.; Michael, L.; Peter, C. Improving the reactivity of hydrazine-bearing MRI probes for in vivo imaging of lung fibrogenesis. Chem. Sci. 2020, 11, 224–231.

40. Meng, Y.; Da, X.; Kadakia, R.T.; Weiran, W.; Que, E.L. Harnessing chemical exchange:F-19 magnetic resonance OFF/ON zinc sensing with a Tm(iii) complex. Chem. Commun. Camb. Engl. 2020, 56, 6257–6260.

41. Xie, D.; Yu, M.; Xie, Z.L.; Kadakia, R.T.; Chung, C.; Ohman, L.E.; Javanmardi, K.; Que, E.L. Versatile Nickel(II) Scaffolds as Coordination-Induced Spin-State Switches for (19) F Magnetic Resonance-Based Detection. Angew. Chem. Int. Ed. Engl. 2020, 59, 22523–22530.

42. Gao, Z.; Hou, Y.; Zeng, J.; Chen, L.; Liu, C.; Yang, W.; Gao, M. Tumor Microenvironment-Triggered Aggregation of Antiphagocytosis (99m) Tc-Labeled Fe3 O4 Nanoprobes for Enhanced Tumor Imaging In Vivo. Adv. Mater. 2017, 29, 1701095.

43. Peng, Q.; Li, Y.; Bo, S.; Yuan, Y.; Yang, Z.; Chen, S.; Zhou, X.; Jiang, Z.X. Paramagnetic nanoemulsions with unified signals for sensitive (19)F MRI cell tracking. Chem. Commun. (Camb.) 2018, 54, 6000–6003.

44. Bo, S.; Yuan, Y.; Chen, Y.; Yang, Z.; Chen, S.; Zhou, X.; Jiang, Z.X. In vivo drug tracking with (19)F MRI at therapeutic dose. Chem. Commun. (Camb.) 2018, 54, 3875–3878.

45. Rajkumar, S.; Prabaharan, M. Multi-functional core-shell Fe3O4@Au nanoparticles for cancer diagnosis and therapy. Colloids Surf. B Biointerfaces 2019, 174, 252–259.

46. Gholipour, N.; Akhlaghi, M.; Kheirabadi, A.M.; Geramifar, P.; Beiki, D. Development of Ga-68 labeled, biotinylated thiosemicarbazone dextran-coated iron oxide nanoparticles as multimodal PET/MRI probe. Int. J. Biol. Macromol. 2020, 148, 932–941.

47. Leszek, J.; Md Ashraf, G.; Tse, W.H.; Zhang, J.; Gasiorowski, K.; Avila-Rodriguez, M.F.; Tarasov, V.V.; Barreto, G.E.; Klochkov, S.G.; Bachurin, S.O.; et al. Nanotechnology for Alzheimer Disease. Curr. Alzheimer Res. 2017, 14, 1182–1189.

48. Azria, D.; Blanquer, S.; Verdier, J.M.; Belamie, E. Nanoparticles as contrast agents for brain nuclear magnetic resonance imaging in Alzheimer's disease diagnosis. J. Mater. Chem. B 2017, 5, 7216–7237.

49. Kieger, A.; Wiester, M.J.; Procissi, D.; Parrish, T.B.; Mirkin, C.A.; Thaxton, C.S. Hybridization-induced "off-on" 19F-NMR signal probe release from DNA-functionalized gold nanoparticles. Small 2011, 7, 1977–1981.

50. Sicilia, G.; Davis, A.L.; Spain, S.G.; Magnusson, J.P.; Boase, N.R.B.; Thurecht, K.J.; Alexander, C. Synthesis of 19F nucleic acid–polymer conjugates as real-time MRI probes of biorecognition. Polym. Chem. 2016, 7, 2180–2191.

51. Pais, A.; Degani, H. Estrogen Receptor-Targeted Contrast Agents for Molecular Magnetic Resonance Imaging of Breast Cancer Hormonal Status. Front. Oncol. 2016, 6, 100.